NiO-Doped Laser-Induced Graphene
A High-Performance Flexible Temperature Sensor

Wang, Shaogang; Tan, Chuanjian; Zong, Qihang; Sett, Avik; Ye, Huaiyu; French, Paddy

DOI
10.1109/SENSORS60989.2024.10784839

Publication date
2024

Document Version
Final published version

Published in
2024 IEEE Sensors, SENSORS 2024 - Conference Proceedings

Citation (APA)
Wang, S., Tan, C., Zong, Q., Sett, A., Ye, H., & French, P. (2024). NiO-Doped Laser-Induced Graphene: A High-Performance Flexible Temperature Sensor. In *2024 IEEE Sensors, SENSORS 2024 - Conference Proceedings* (Proceedings of IEEE Sensors). IEEE.
https://doi.org/10.1109/SENSORS60989.2024.10784839

NiO-Doped Laser-Induced Graphene: A High-Performance Flexible Temperature Sensor

Shaogang Wang [1], Chuanjian Tan [1], Qihang Zong [2], Avik Sett [1], Huaiyu Ye [2], and Paddy French [1,*]

[1] Faculty of EEMCS, Delft University of Technology, Mekelweg 4, 2628 CD Delft, The Netherlands.

[2] School of Microelectronics, Southern University of Science and Technology, Shenzhen 518055, China.

[*]E-mail: p.j.french@tudelft.nl

***Abstract*—This study introduces a high-performance flexible temperature sensor prepared using laser-induced graphene (LIG) doped with nickel oxide (NiO) nanoparticles (NPs). Unlike conventional LIG surface doping methods, we developed a nickel oxide-doped LIG flexible temperature sensor by introducing NiO NPs into a polyimide (PI) precursor solution cured into a film followed by ultraviolet (UV) laser treatment. This approach achieves a more stable and uniform doping process while further improving the sensing performance of LIG-based temperature sensors. Over a prospective temperature detection range (30-100 °C), the sensitivity of the NiO-doped LIG temperature sensor is significantly improved from -0.064% $°C^{-1}$ to -0.079% $°C^{-1}$, an improvement of 19.3%, compared to that of the intrinsic LIG temperature sensor, while maintaining high linearity (R^2 = 0.999) as well as excellent temperature stability and reliability. This research not only enhances the performance of flexible temperature sensors based on LIG but also paves new pathways for its industrial production in various application fields.**

Keywords*—LIG; NiO NPs; Flexible Temperature Sensors; UV laser

I. Introduction

Temperature is a fundamental physical quantity that describes the thermal state of an object, measuring the average change in internal thermal energy over time and space. Temperature sensors, by monitoring the temperature of objects and environments, have become one of the most essential measurement tools in the fields of science and engineering. With continual advancements in technology, high-precision temperature detection techniques are crucial for enhancing the quality of medical diagnostics and environmental monitoring [1, 2]. Additionally, the rapid development of flexible electronics and the increasing demand for wearable devices have driven higher performance standards for flexible temperature sensors [3]. Based on their working principles, flexible temperature sensors can be broadly categorized into three types: resistive [4, 5], thermocouple [6, 7], and thermistor [8, 9]. Among these, resistive temperature sensors are renowned for their high accuracy, stability, and excellent linear response across a wide temperature range [10].

In the material research of resistive flexible temperature sensors, graphene has attracted considerable interest due to its expectational electrical conductivity [11], excellent biocompatibility [12], and outstanding chemical stability [13]. Laser-induced graphene (LIG) technology enables the preparation and modulation of graphene through precise non-contact processing at room temperature [14, 15]. The flexibility, controllability, and efficiency of this method accelerate its further development [16]. In LIG-based temperature sensors, the mechanism of operation relies on the sensitivity of the resistance to temperature changes. As the temperature increases, the carriers in the graphene are thermally excited and increase, causing a change in resistance. Meanwhile, temperature fluctuations affect phonon scattering within the graphene lattice, further altering the resistance [17]. As reported, Marengo et al. [18] have designed a flexible temperature sensor using LIG technology, which shows a nonlinear negative temperature coefficient (NTC) response within the 20 to 60 °C range, with a resistance decrease of 0.1% (NTC = -0.1% $°C^{-1}$). Additionally, Baek et al. [19] have fabricated sensors using polyimide films that achieve a highly linear response within the 0 to -150 °C range, with an R^2 of 0.99238. Furthermore, Zhang et al. [20] developed a high-performance LIG-based temperature sensor that exhibits a sensitivity of 0.05% $°C^{-1}$ and linearity of 0.999, with response and recovery times of 2.0s and 3.9s, respectively, across a temperature range of 30 to 100 °C. These innovative studies demonstrate that using LIG technology to fabricate flexible temperature sensors is a highly effective strategy.

Herein, we used an innovative approach to prepare flexible temperature sensors by uniformly doping nickel oxide (NiO) nanoparticles in a polyimide (PI) precursor solution and forming doped LIGs by ultraviolet (UV) laser treatment. Unlike the traditional surface doping method, we started the doping from the preparation stage of PI film, which not only facilitates industrialized production but also significantly improves the doping uniformity and the stability of the sensor. With this technique, we successfully improved the sensitivity of the temperature sensor from the original -0.064% $°C^{-1}$ to -0.079% $°C^{-1}$, an increase of 19.3%, while maintaining high linearity (R^2 = 0.99) and excellent temperature stability. This study not only improves the performance of LIG-based flexible temperature sensors but also opens up new possibilities for the further development and application of LIG-based temperature sensing technology.

II. Experimental Section

Fig. 1 illustrates the schematic diagram of the fabrication process for the flexible temperature sensors based on NiO-doped LIG. The entire fabrication process consists of 8 main steps. In Step 1, 1.5 g of NiO nanoparticles (NPs) were ultrasonically dispersed in 2.0 g

2024 IEEE SENSORS | 979-8-3503-6351-7/24/$31.00 ©2024 IEEE | DOI: 10.1109/SENSORS60989.2024.10784839

of DMF solvent, followed by the addition of 6.5 g of PI precursor solution, which was thoroughly mixed using a planetary mixer (2000 rpm and 60 seconds). In Step 2, the prepared paste was spin-coated at 1000 rpm for 30 seconds on a 4-inch wafer pre-coated with a PSSNa sacrificial layer. In Step 3, the wafer was heated on a hotplate to induce the curing of the paste into a NiO-doped PI film. In Step 4, a 0.12 mm thick PI tape was applied using a squeegee to the already cured doped PI film to ensure stable mechanical properties. In Step 5, the doped PI film adhered to the PI tape was ultrasonically delaminated in deionized water using a high-power ultrasonic cleaner and then dried in an oven at 60 °C for 20 minutes. In Step 6, a UV laser system was used to mass-fabricate the LIG temperature sensing region with a continuous linear structure on the NiO-doped PI layer. In Step 7, screen printing technology was used to prepare corresponding silver electrodes at both ends of the already prepared LIG sensing regions. Finally, in Step 8, the fabricated flexible temperature sensors were sliced and packaged.

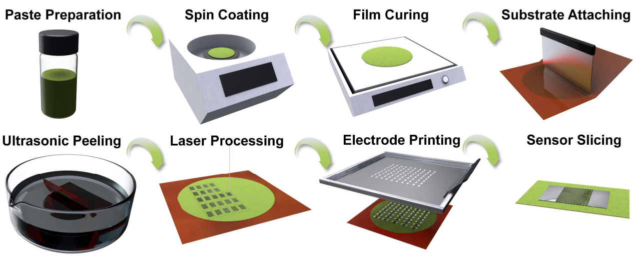

Fig. 1. Schematic illustration of the fabrication process for NiO-doped LIG flexible temperature sensor.

The LIG sensing region was fabricated using an ultraviolet (UV) pulsed laser system (Grace X 355-3A, Han's Laser Technology Industry Group Co., Ltd., wavelength: 355 nm). The laser scan speed was set at 10 mm/s, and the motion in the *X-Y* direction was precisely controlled by software. The distance between the field lens and the sample was adjusted using the vertical *Z*-direction translation stage. To achieve high LIG fabrication quality, the laser repetition frequency and laser power were set at 200 kHz and 0.6 W.

The change in resistance of the flexible temperature sensor over the range of 30 to 100 °C was measured during the experiments using a hotplate covered with a Faraday cage. The resistance and temperature are accurately measured and captured by a computationally controlled digital source meter (Keithley 2450 SMU) and a hotplate (Asone-NDK-1A) repetitively. Temperature variations are continuous, and quasi-equilibrium conditions are ensured.

The Temperature of resistance (TCR), as the key parameter for measuring temperature sensors, is determined by:

$$\mathrm{TCR} = \frac{R_{\mathrm{T}}\text{-}R_0}{R_0 \cdot (T\text{-}T_0)} \times 100\% = \frac{\Delta R}{R_0 \cdot \Delta T} \times 100\% \qquad (1)$$

where the R_0 and R_T represent the resistance of the sensor at T_0 (30 °C) and the tested temperature of T, respectively [21]. All temperature test experiments were conducted at 25 °C room temperature and 30% relative humidity (RH).

III. Result and Discussion

A. Characterization of LIG Doped with NiO NPs

The conversion of NiO-doped polyimide (PI) films into laser-induced graphene (LIG) is achieved through UV laser irradiation with optimized parameters. During the linear scanning of the laser, the PI film is rapidly and locally heated by the laser (temperatures exceeding 2500 °C), causing the aromatic compounds to rearrange into a graphite structure. During this process, the high temperature breaks the imide rings. It generates volatile gases while transforming the aromatic and conjugated structures into an sp^2 hybridized layer carbon network, ultimately forming a graphene lattice [22]. The porous structure of the NiO-doped LIG surface was characterized using scanning electron microscopy (SEM), as shown in Fig. 1(a).

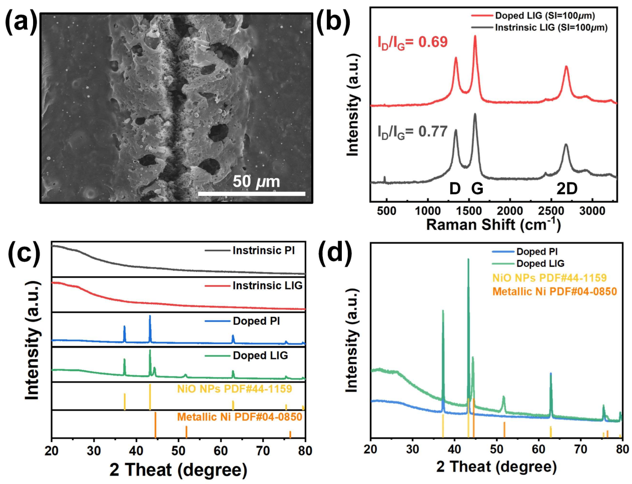

Fig. 2. (a) SEM image of the porous structure of NiO-doped LIG on the surface of the PI film. (b) Comparison of Raman spectra of intrinsic LIG and NiO doped LIG. (c) and (d) XRD spectra of intrinsic PI, intrinsic LIG, NiO-doped PI, and NiO-doped LIG. (d) Comparison of the magnified XRD patterns of NiO-doped PI and NiO-doped LIG.

Further, Raman spectroscopy was employed to reveal the structural characteristics of the material before and after the doping of NiO NPs into LIG, as shown in Fig. 2(b). The spectra of the UV laser-treated PI films exhibited three prominent peaks (D, G, and 2D peaks) near 1350, 2580, and 2690 cm^{-1}, respectively. Among them, the D peak indicates a hybridized vibrational mode of the disordered sp^2-hybridized graphitic structure, which is activated by defects corresponding to the double resonance processes [23]. The G peak, indicative of a graphite-derived structure, arises from the vibrations of sp^2 carbon atoms arranged in a hexagonal plane [24]. The 2D peak results from second-order resonance, signifying the complete graphitization of the PI film [25]. Correspondingly, the I_D/I_G ratio typically confirms the graphitization degree and the crystalline quality of the LIG after laser treatment [26]. Interestingly, the quality of LIG prepared from polyimide (PI) films doped with NiO NPs is significantly improved after laser treatment using optimized laser parameters, as evidenced by an increase in the I_D/I_G. This suggests that the doping of NiO NPs promotes a more ordered reorganization of carbon atoms and further improves the graphitization level of LIG.

To further reveal the material transformation of LIG before and after laser treatment, X-ray diffraction (XRD) was used to analyze the evolution of the material crystal structure, as shown in Fig. 2(c) and Fig. 2(d). Overall, the intrinsic PI films show no prominent diffraction peaks before and after laser treatment, reflecting their amorphous carbon properties. However, the XRD spectra of the NiO-doped PI films show characteristic peaks of NiO, especially at 37.2°, 43.4°, 62.9°, and 75.4°, corresponding to the (101), (110), (104), and (113) crystal planes of NiO (PDF#44-1159), respectively. Crucially, after laser treatment, the NiO-doped PI films not only exhibit the characteristic peaks of NiO but also show peaks indicative of metallic nickel, located at 44.5°, 51.8°, and 76.4°, corresponding to the (111), (200), and (220) crystal planes of Ni (PDF#04-0850), respectively. These results clearly demonstrate that the UV laser treatment process not only successfully converted PI to LIG but also facilitated the slight reduction of NiO to Ni metal, suggesting the generation of oxygen vacancy defects. These results demonstrate that the use of laser-induced techniques for the direct preparation of metal- and metal oxide-doped graphene provides experimental solid support, demonstrating the great potential of this technique for the preparation of functional nanocomposites.

B. Performance Testing of Temperature Sensors

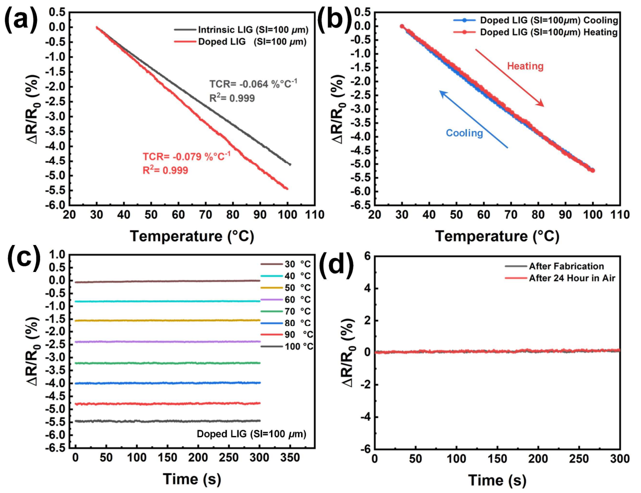

Fig. 3. (a) Comparison of relative resistance versus temperature curves of LIG-based temperature sensors before and after NiO doping (Scanning interval = 100 μm). (b) Relative resistance change of doped LIG temperature sensors during cooling and heating cycles. (c) Stability test of resistance changes over time at different temperatures for NiO-doped LIG-based temperature sensors. (d) Comparison of curves before and after a 24-hour long-term air stability test for NiO-doped LIG flexible temperature sensors.

The performance of the prepared flexible temperature sensors was measured over the temperature range of 30 to 100 °C, exhibiting broad temperature sensing behavior, as shown in Fig. 3(a). The flexible temperature sensors of both intrinsic LIG and NiO-doped LIG demonstrated excellent linear responses to temperature with coefficients of determination (R^2) of 0.999, which indicates a good fit to the experimental data and also proves the practical application value. Notably, the NiO-doped LIG sensor exhibits a negative coefficient of resistance (NTCR) of -0.079% °C^{-1}, which is a 23% improvement in sensitivity compared to the sensitivity of the intrinsic LIG sensor (-0.064% °C^{-1}). Additionally, within the temperature range of 30 to 100 °C, the NiO-doped LIG sensor showed extremely high consistency during both heating and cooling phases, as shown in Fig. 3(b). Furthermore, the NiO-doped LIG temperature sensor maintained excellent stability over a 5-minute continuous test period at a fixed temperature in the 30 to 100 °C temperature range (10 °C intervals), as shown in Fig. 3(c). Meanwhile, the NiO-doped LIG sensor exhibits stable electrical performance after 24 hours in an atmospheric condition, as shown in Fig. 3(d). The sensitivity of the prepared sensor is significantly higher than that of previous LIG-based temperature sensors (0.041% °C^{-1} within 30-40 °C and 0.05% °C^{-1} within 30-100 °C) [20, 27].

C. Sensing Mechanism of Temperature Sensors

As a graphene-like material, LIG exhibits negative temperature coefficient (NTC) characteristics due to its unique graphene structure and electron transport properties [28]. As the temperature increases, thermal excitation allows more electrons to gain enough energy to jump from the valence band (VB) to the conduction band (CB), thus significantly increasing the electron density in the conduction band [29]. This process further increases the number and mobility of carriers, leading to a decrease in the overall resistance of the LIG and thus exhibiting a negative temperature coefficient resistance characteristic. After laser treatment, the introduced NiO nanoparticles are partially reduced to metallic Ni while corresponding oxygen vacancy defects are generated. The conductive network formed by metallic Ni and the defect energy levels introduced by the oxygen vacancy defects significantly contribute to the hopping transport of carriers when the temperature increases [30]. As a result, the NiO-doped LIG resistance is significantly reduced when the temperature is increased, which further enhances the sensitivity of the NiO-LIG temperature sensor.

IV. Conclusion

In this study, we successfully developed a high-performance flexible temperature sensor by doping NiO nanoparticles into LIG using UV laser treatment. This innovative doping technique, initiated at the PI film preparation stage, significantly improved the uniformity and stability of the sensors. The NiO-doped LIG sensors exhibited a remarkable sensitivity increase of 19.3%, achieving a sensitivity of -0.079% °C^{-1} and maintaining high linearity (R^2 = 0.999). The sensors demonstrated excellent stability and consistency over a prospective temperature range (30 to 100 °C), highlighting their potential for practical applications in flexible electronics and wearable devices. The results of this study provide a solid foundation for the further development and industrial production of advanced LIG-based temperature sensing technologies.

REFERENCING

[1] T. R. Ray et al., "Bio-integrated wearable systems: a comprehensive review," Chemical reviews, vol. 119, no. 8, pp. 5461-5533, 2019.

[2] B. A. Kuzubasoglu and S. K. Bahadir, "Flexible temperature sensors: A review," Sensors and Actuators A: Physical, vol. 315, p. 112282, 2020.

[3] Y. Su et al., "Printable, highly sensitive flexible temperature sensors for human body temperature monitoring: a review," Nanoscale research letters, vol. 15, pp. 1-34, 2020.

[4] G. Rajan et al., "Low operating voltage carbon–graphene hybrid E-textile for temperature sensing," ACS applied materials & interfaces, vol. 12, no. 26, pp. 29861-29867, 2020.

[5] H. Qin et al., "Laser-Induced Graphene-Based Smart Textiles for Wireless Cross-Body Metrics," ACS Applied Nano Materials, vol. 6, no. 20, pp. 19158-19167, 2023.

[6] D. Assumpcao, S. Kumar, V. Narasimhan, J. Lee, and H. Choo, "High-performance flexible metal-on-silicon thermocouple," Scientific reports, vol. 8, no. 1, p. 13725, 2018.

[7] M. M. Mallick et al., "High‐Sensitivity Flexible Thermocouple Sensor Arrays Via Printing and Photonic Curing," Advanced Functional Materials, p. 2301681, 2023.

[8] J. Shin et al., "Sensitive wearable temperature sensor with seamless monolithic integration," Advanced Materials, vol. 32, no. 2, p. 1905527, 2020.

[9] Z. Peng et al., "Flexible Copper-Based Thermistors Fabricated by Laser Direct Writing for Low-Temperature Sensing," ACS Applied Materials & Interfaces, 2024.

[10] Q. Li, L. N. Zhang, X. M. Tao, and X. Ding, "Review of flexible temperature sensing networks for wearable physiological monitoring," Advanced healthcare materials, vol. 6, no. 12, p. 1601371, 2017.

[11] Z.-S. Wu et al., "Synthesis of graphene sheets with high electrical conductivity and good thermal stability by hydrogen arc discharge exfoliation," ACS nano, vol. 3, no. 2, pp. 411-417, 2009.

[12] Z. Xiong et al., "Harnessing the 2D Structure‐Enabled Viscoelasticity of Graphene‐Based Hydrogel Membranes for Chronic Neural Interfacing," Small Methods, vol. 6, no. 5, p. 2200022, 2022.

[13] R. Stine, W.-K. Lee, K. E. Whitener Jr, J. T. Robinson, and P. E. Sheehan, "Chemical stability of graphene fluoride produced by exposure to XeF2," Nano letters, vol. 13, no. 9, pp. 4311-4316, 2013.

[14] Z. Li, L. Huang, L. Cheng, W. Guo, and R. Ye, "Laser‐Induced Graphene‐Based Sensors in Health Monitoring: Progress, Sensing Mechanisms, and Applications," Small Methods, p. 2400118, 2024.

[15] J. Lin et al., "Laser-induced porous graphene films from commercial polymers," Nature communications, vol. 5, no. 1, p. 5714, 2014.

[16] L. Huang, J. Su, Y. Song, and R. Ye, "Laser-induced graphene: En route to smart sensing," Nano-micro letters, vol. 12, pp. 1-17, 2020.

[17] S. Gandla et al., "Highly linear and stable flexible temperature sensors based on laser‐induced carbonization of polyimide substrates for personal mobile monitoring," Advanced Materials Technologies, vol. 5, no. 7, p. 2000014, 2020.

[18] M. Marengo, G. Marinaro, and J. Kosel, "Flexible temperature and flow sensor from laser-induced graphene," in 2017 IEEE SENSORS, 2017: IEEE, pp. 1-3.

[19] S. Baek, J. Kim, P. Pujar, H. J. Kwon, S. Kim, and S. Gandla, "Sub‐zero temperature sensor based on laser‐written carbon," Advanced Electronic Materials, vol. 8, no. 7, p. 2101252, 2022.

[20] Y. Zhang et al., "High-linearity graphene-based temperature sensor fabricated by laser writing," Journal of Materials Science: Materials in Electronics, vol. 35, no. 2, p. 109, 2024.

[21] A. Chhetry et al., "Black phosphorus@ laser‐engraved graphene heterostructure‐based temperature–strain hybridized sensor for electronic‐skin applications," Advanced Functional Materials, vol. 31, no. 10, p. 2007661, 2021.

[22] H. Wang, Z. Zhao, P. Liu, and X. Guo, "A soft and stretchable electronics using laser-induced graphene on polyimide/PDMS composite substrate," npj Flexible Electronics, vol. 6, no. 1, p. 26, 2022.

[23] L. G. Cançado et al., "Quantifying defects in graphene via Raman spectroscopy at different excitation energies," Nano letters, vol. 11, no. 8, pp. 3190-3196, 2011.

[24] T. Kuila, S. Bose, A. K. Mishra, P. Khanra, N. H. Kim, and J. H. Lee, "Chemical functionalization of graphene and its applications," Progress in Materials Science, vol. 57, no. 7, pp. 1061-1105, 2012.

[25] A. C. Ferrari et al., "Raman spectrum of graphene and graphene layers," Physical review letters, vol. 97, no. 18, p. 187401, 2006.

[26] L. Cançado et al., "General equation for the determination of the crystallite size La of nanographite by Raman spectroscopy," Applied physics letters, vol. 88, no. 16, 2006.

[27] H. Kun, L. Bin, M. Orban, Q. Donghai, and Y. Hongbo, "Accurate flexible temperature sensor based on laser-induced graphene material," Shock and Vibration, vol. 2021, pp. 1-7, 2021.

[28] Y. Li, H. Nakamura, D. H. Lee, Y. Qin, Y. Xuan, and K. Takei, "Temperature Coefficient of Resistance of Transferred Laser-Induced Graphene," ACS Applied Electronic Materials, 2024.

[29] Y. Lu et al., "Robust Fiber‐Shaped Flexible Temperature Sensors for Safety Monitoring with Ultrahigh Sensitivity," Advanced Materials, p. 2310613, 2024.

[30] T. Wang et al., "A Highly Sensitive NiO Flexible Temperature Sensor Prepared by Low-Temperature Sintering Electrohydrodynamic Direct Writing," Micromachines, vol. 15, no. 9, p. 1113, 2024.